PERGAMON

International Journal of Heat and Mass Transfer 43 (2000) 1617–1627

International Journal of HEAT and MASS TRANSFER

www.elsevier.com/locate/ijhmt

Convective stability of a particle-laden fluid system in the presence of solidification

Calvin Mackie*

Tulane University, School of Mechanical Engineering, New Orleans, LA 70118, USA

Received 10 December 1998; received in revised form 29 June 1999

Abstract

In many phase transformation processes, natural convection controls the freezing or melting rate of the material. The kinematics of the solid–liquid interface, which are coupled with bulk convection in the melt, play an important role in determining the microstructure of a solidified material. Although the fundamental problem of thermoconvective instability of a single-component in a horizontal liquid layer has been studied extensively, there still exist additional complexities which arise during solidification due to the presence of nonmelting components. This study addresses the problem of Rayleigh–Bénard instability of a liquid layer in the presence of suspended particles undergoing a phase transformation. A linear stability analysis determined the effects of the particles and phase-change on the conditions for incipient convection. The analysis reveals that the concentration of and heat transfer between particles affect the stability of the system.

Keywords: Natural convection; Stability; Suspended particles; Solidification; Freezing; Phase change

1. Introduction

It is recognized that fluid mechanics, in general, and buoyancy-driven flows, in particular, play a critical role in determining interfacial traits of a solidifying material; fluid motion adjacent to a solidifying interface affects the local thermal and solutal fields which control the geometric, dynamic and thermodynamic characteristics of the interface [1,2]. For instance, convection during fabrication or solidification processing of cast metal matrix composites affects the distribution of particulates in the composites, in turn influencing the properties of the material. During the past two decades, there has been great interest in establishing the role of thermal convection in processes undergoing phase change. Phase transformation from liquid to solid (or vice versa) is a phenomenon central to a wide range of manufacturing and natural processes. More recently, the growth of crystals from melt or other solidifying aqueous solutions in the materials processing industry has generated a considerable number of investigations in phase change phenomena.

Although thermoconvective instability in a horizontal fluid layer driven by buoyancy effects has been studied extensively [3–5], there exist additional unresolved complexities associated with processing of mixtures due to the presence of a nonmelting component. This fundamental study addresses hydrodynamic stability issues during solidification of such

* Tel.: +1-504-865-5137; fax: +1-504-865-5345..

E-mail address: cmackie@mailhost.tcs.tulane.edu (C. Mackie).

0017-9310/00/$ - see front matter
PII: S0017-9310(99)00226-4

Nomenclature

C_L	Specific heat capacity of liquid at constant pressure
C_P	Specific heat capacity of particles at constant pressure
D	Differential operator
f	Temperature perturbation variable
$\lambda = 2\pi/k_c$	Wavelength of the incipient convection cells
$\vec{g}$	Gravitational acceleration vector
g	Perturbation variable for the solid temperature
h	The particle heat transfer coefficient, $h = 2\kappa_p/r$
k	Separation constant or wave number
L	Length of the solidification system
L_1	$(\rho_p/\rho_L)(\partial/\partial_t)-\Omega_2$
L_2	$(\partial/\partial_t)+1$
L_3	$(\partial/\partial_t)-1$
N_0	Number density of particles
$\vec{n}$	Unit normal vector
P	Pressure
Pr	Prandtl number
q	k^2
r	Constant particle radius
Ra	Rayleigh number
R_c	Critical Rayleigh number for system with particles
Ra_c	Critical Rayleigh number for system absence of particles
s	Vertical component of particle velocity, v
St	Stefan number
$\vec{t}_i$	Tangential vectors on the interface, $i = 1, 2$
T_1	Temperature of upper rigid plate on general solidification model
T_o	Temperature of lower rigid plate on general solidification model
T_M	Interface melting temperature
u	Velocity vector for liquid, $u = u(u, v, w)$
v	Velocity vector for particles, $v = v(r, x, s)$
w	Velocity component in the z-direction for the liquid
$\hat{w}$	Vertical velocity perturbation variable
x	First Cartesian direction
y	Second Cartesian direction
ΔT_L	Temperature difference across the porous layer
∇	Gradient operator
$\nabla\cdot$	Divergence operator
∇^2	Laplacian operator

Greek symbols

α	Ratio of the liquid thermal diffusivity to the solid
α_L	Thermal diffusivity of the bulk liquid region
α_S	Thermal diffusivity of the solidified region
Λ	Solid–liquid aspect ratio, L_s/L_L
β	Coefficient of volumetric thermal expansion
γ	Bulk concentration density of particles
σ	Complex growth rate
Γ	Particle aspect ratio, r/η_0
H_{SL}	Latent heat per unit area of solid
κ	Thermal conductivity
K	$6\pi\mu_L r$
η	Interface position coordinate
$\hat{\eta}$	Normalized perturbation variable for the interface position
η_0	Length of the liquid region
η_t	Time rate of change of the interface
μ_L	Dynamic viscosity of the liquid region
ν_L	Kinematic viscosity of the liquid
ρ	Ratio of the density of the liquid to the solid
ρ_L	Density of the liquid region
ρ_S	Density of the solidified region
σ	Real part of the complex growth rate, s
Φ	Pattern planform
φ	Heat loading, $[\rho_p c_p \gamma]/[\rho_L c_L(1-\gamma)]$
Ω_1	$(4\pi r^2 N_0 h)/(\rho_L c_L \alpha_L)$
Ω_2	$6\pi r N_0$
Ω_3	$(4\pi r^2 N_0 h)/(\rho_p c_p \alpha_L)$

Subscripts

b	Basic state
c	Critical
f	Fluid
L	Liquid
p	particle
s	Solid
o	Reference or equilibrium
0, 1, 2, 3, ...	Sequence of functions or constants

Superscripts

$\rightarrow$	Vector
$'$	Perturbation
$\hat{}$	Normal mode perturbation
$*$	Nondimensional perturbation
–	Basic state (overbar)

mixtures by modeling the solid–liquid slurry of a composite mixture as a particle-laden horizontal liquid layer solidifying in a gravitational field. One of the main difficulties of studying the solid–liquid slurry is that physically, the particulates are not suspended in a homogeneous fashion; however, their subsequent motion or settling presents another important problem beyond the scope of this investigation. The settling event in the production of particulate metal matrix composites evolves by the dynamic and thermodynamic interactions with the solidification process rather than prior to it [6]. Consequently, such parameters as the solidification rate, convection, thermal characteristics, geometry of reinforcement or particles all affect the hydrodynamic and thermodynamic interactions during solidification and must be considered for the optimization of the production of such materials. Thus, this analytical study focuses on the effects of nonmelting suspended particles and phase change on incipient convection.

The conditions for the onset of buoyancy driven convection during the heating of a liquid layer from below were initially treated experimentally by Bénard in 1900 and theoretically by Rayleigh in 1916 [5]. Since then, various facets of this problem have been examined and practical applications abound. Theoretical investigations of the Bénard problem incorporating suspended particles have shown that the presence of the particles acts to destabilize the system [7]. Neglecting thermal interactions between the particles and particle buoyancy, the authors demonstrated that the decrease in stability was due solely to the additional heat capacity of the particles. Recent studies [8,9] have incorporated fluid–particle thermal interaction and demonstrated the effect on the stability of the system. Theoretical examination of such a Bénard system, independent of particles with freezing from above, indicates that the presence of solidification also acts to decrease the convective stability of the system [10]. A recent study by the author illustrated that the solidification and boundary conditions in a particle-laden system greatly affect the onset of convection [11]. In this paper, a manifestation of the fluid–particle laden system, which consists of a partially solidified material enclosed between two parallel horizontal boundaries, is considered.

This study focuses on the effect of particle thermal interactions, particle buoyancy, heat loading, solid–thickness ratio and volume fraction on the incipient convection in the interstitial liquid. By parametrically changing the aforementioned parameters, a greater understanding of the influence of such variables on the convective stability of a particle-laden mixture was ascertained.

2. Problem formulation

A quiescent horizontal layer of a pure fluid in a gravitational field heated from below will not always remain so in the presence of an adverse density gradient beyond a threshold value capable of giving rise to fluid motion. This observation may be applied to examine the solidification of a particle-laden liquid layer enclosed between two rigid, parallel, thermally dissimilar, horizontal plates of infinite extent, a distance L apart, in a gravitational field as shown in Fig. 1. The analytical model is formulated under the assumptions that the liquid layer is heated from below and cooled from above such that the liquid in the upper part of the layer is frozen, and the effective thermophysical and transport properties of the system are homogeneous and isotropic. Fluid motion within the layer is described via a Newtonian, Boussinesq model of the Navier Stokes equations. Motion due to density change upon phase change is negligible. The melt–freeze front is assumed to be a thin surface of negligible thickness that remains at the melting point of the phase-change material. The temperature at the bottom plate is maintained such that the melting temperature, T_M, is bounded between the lower plate constant temperature, T_o, and the upper plate constant temperature, T_l ($T_o > T_M > T_l$). Therefore, there is a solid–liquid interface at $z=\eta_o$, $0 < \eta_o < L$ (Fig. 1). Buoyancy force on the particles is considered and inter-particle interaction is negligible under the assumption that the distance between particles is quite large compared with their diameter, however, fluid–particle thermal exchange is taken into account. The presence of the particles in the liquid manifests as an extra force term in the equations of motion for the particles and the governing liquid momentum equation. As such, the force exerted on the liquid by the particles is equal and opposite to that exerted by the particles on the liquid. Since there exists no bulk motion in the solid, the temperature field within the solidified layer is described by the thermal energy equation

$$\frac{\partial T_s}{\partial t} = \alpha_s \nabla^2 T_s. \tag{1}$$

For the liquid, the temperature field may be obtained from a simultaneous solution of the thermal energy and continuity equations, together with the modified Boussinesq model of the momentum equation. These are expressed, respectively, as

$$\rho_L c_L (1-\gamma)\left[\frac{\partial}{\partial t} + \vec{u}\cdot\nabla\right] T_L = 4\pi r^2 N h (T_p - T_L) + \kappa_L \nabla^2 T_L, \tag{2}$$

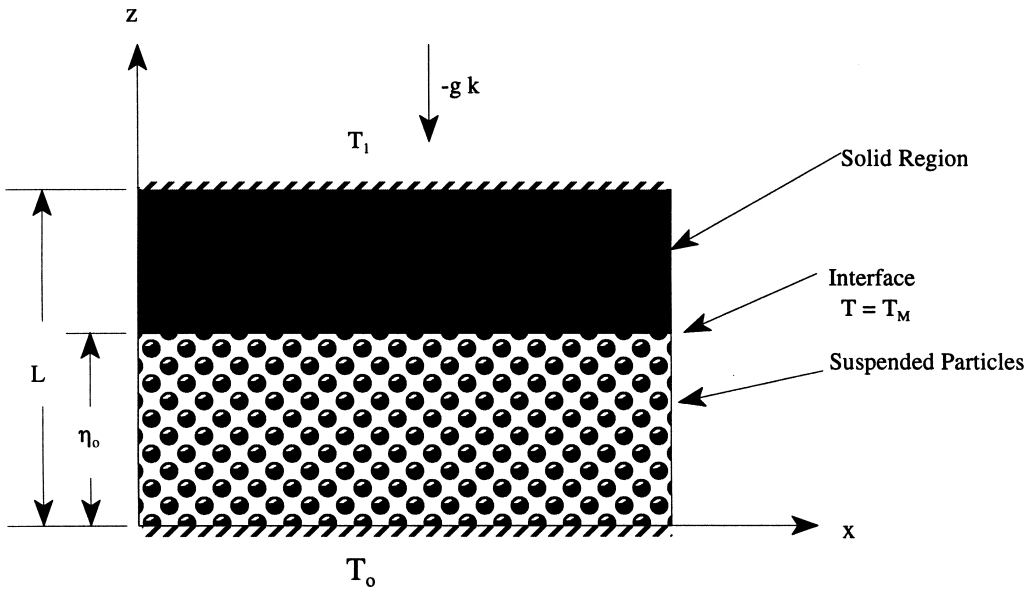

Fig. 1. Solidification model for particle-laden mixture.

$$\nabla \cdot \vec{u} = 0 \tag{3}$$

and

$$\rho_L(1-\gamma)\left[\frac{\partial}{\partial t} + (\vec{u}\cdot\nabla)\right]\vec{u} = -(1-\gamma)\nabla P + \rho_L(1-\gamma)\beta(T_L - T_{ref})\vec{g}\cdot\vec{k} + \mu_L(1-\gamma)\nabla^2\vec{u} + KN(\vec{v}-\vec{u}). \tag{4}$$

The equations of motion and continuity for the particles are

$$\rho_P c_P \gamma\left[\frac{\partial}{\partial t} + \vec{v}\cdot\nabla\right]T_L = 4\pi r^2 Nh(T_p - T_L), \tag{5}$$

$$\nabla \cdot \vec{v} = 0 \tag{6}$$

and

$$\rho_P\gamma\left[\frac{\partial}{\partial t} + (\vec{v}\cdot\nabla)\right]\vec{v} = \rho_L\gamma\beta(T_L - T_{ref})\vec{g}\cdot\vec{k} + KN(\vec{u}-\vec{v}). \tag{7}$$

The boundary conditions on the interface are the continuity of temperature,

$$T_L = T_s = T_M, \tag{8}$$

where the interface curvature due to undercooling of the melt is neglected, and the conservation of energy,

$$\rho_s H_{sL}\frac{\partial \eta}{\partial t} = |k_s\nabla T_s - k_L\nabla T_L|\cdot\vec{n}. \tag{9}$$

Also defined on the interface is the conservation of mass (kinematic condition),

$$\rho_L(\vec{u}\cdot\vec{n}) = (\rho_L - \rho_s)\frac{\partial\eta}{\partial t}\vec{k}\cdot\vec{n} \tag{10}$$

and the no-slip condition,

$$\vec{u}\cdot\vec{t}_1 = \vec{u}\cdot\vec{t}_2. \tag{11}$$

The temperatures on the bounding surfaces are constant,

$$@z = 0,\ T_L = T_0 \text{ and } @z = 1,\ T_s = T_1. \tag{12}$$

3. Stability analysis

Initially, the stationary system is in a static equilibrium state with no fluid or particle motion and a planar interface at $z=\eta_o$. The pertinent variables, u (and v), x (and y, z), t and p are normalized, respectively, as α_L/η_0, η_0, η_0^2/α_L, and $(\rho_L v_L \alpha_L)/\eta_0^2$.

The basic state under consideration is that of a stagnant layer of liquid (no settling), with a hydrostatic pressure distribution, a uniform particle distribution, and a purely conductive temperature distribution. In normalized form, the basic state becomes (denoted by variables with bars on top),

$$\bar{v}=0,\quad \bar{u}=0,\quad \frac{\mathrm{d}\bar{p}}{\mathrm{d}z}=Ra\bar{T}_{\mathrm{L}}\cdot\vec{k},\quad \bar{T}_{\mathrm{L}}=1-z,\qquad \bar{T}_{\mathrm{s}}=\frac{1}{1-L^{*}}(1-z), \tag{13}$$

where $\bar{T}_{\mathrm{s}}$ is defined between the limits of $z=1$ and $L^{*}=L/\eta_{\mathrm{o}}$. The basic state perturbations representing the response due to a slight freezing of the system are defined as

$$\vec{u}=u',\quad \vec{v}=v',\quad \eta=1+\eta',\quad T_{\mathrm{s}}=\bar{T}_{\mathrm{s}}+T'_{\mathrm{s}},\qquad T_{\mathrm{L}}=\bar{T}_{\mathrm{L}}+T'_{\mathrm{L}},\quad p=\bar{p}+p'. \tag{14}$$

Substituting these expressions into the governing equations and linearizing in the disturbance quantities, yields: for the solid

$$\frac{\partial T'_{\mathrm{s}}}{\partial t}=\frac{\alpha_{\mathrm{s}}}{\alpha_{\mathrm{L}}}\nabla^{2}T'_{\mathrm{s}}, \tag{15}$$

for the liquid

$$(1-\gamma)\left[\frac{\partial T'_{\mathrm{L}}}{\partial t}-w'\right]=\Omega_{1}(T'_{\mathrm{p}}-T'_{\mathrm{L}})+(1-\gamma)\nabla^{2}T'_{\mathrm{L}}, \tag{16}$$

$$\nabla\cdot u'=0 \tag{17}$$

and

$$Pr^{-1}(1-\gamma)\left[\frac{\partial u'}{\partial t}+(u'\cdot\nabla)u'\right]=-(1-\gamma)\nabla p'+(1-\gamma)RaT'_{\mathrm{L}}\cdot\vec{k}+(1-\gamma)\nabla^{2}u'+\Omega_{2}(u'-v'), \tag{18}$$

where w' is the vertical component of the perturbation velocity, $\vec{u}'$. The governing disturbance equations for the particles are

$$\gamma\left[\frac{\partial T'_{\mathrm{p}}}{\partial t}+v'\cdot\nabla\bar{T}_{\mathrm{L}}\right]=\Omega_{3}(T'_{\mathrm{L}}-T'_{\mathrm{p}}), \tag{19a}$$

$$\nabla\cdot v'=0, \tag{19b}$$

$$\gamma Pr^{-1}\frac{\rho_{\mathrm{p}}}{\rho_{\mathrm{L}}}\frac{\partial v'}{\partial t}=\gamma RaT'_{\mathrm{L}}\cdot\vec{k}+\Omega_{2}(v'-u'). \tag{19c}$$

The linearized boundary conditions on the interface ($z=1$) for the perturbation model are

$$T'_{\mathrm{s}}=-\eta'\frac{\partial\bar{T}_{\mathrm{s}}}{\partial z},\quad T'_{\mathrm{L}}=-\eta'\frac{\partial\bar{T}_{\mathrm{L}}}{\partial z}, \tag{20}$$

$$u'=(1-\rho)\eta'_{x},\quad v'=(1-\rho)\eta'_{y},\quad w'=(1-\rho)\eta'_{t} \tag{21}$$

and

$$\rho StPr\frac{\partial\eta'}{\partial t}=\Lambda\frac{\partial T'_{\mathrm{s}}}{\partial z}-\frac{\partial T'_{\mathrm{L}}}{\partial z}. \tag{22}$$

Appearing in the energy equation is the nondimensional parameter:

$$\Lambda=\frac{L-\eta_{0}}{\eta_{0}}=\frac{L_{\mathrm{s}}}{L_{\mathrm{L}}}=\frac{k_{\mathrm{s}}\Delta T_{\mathrm{s}}}{k_{\mathrm{L}}\Delta_{\mathrm{L}}}, \tag{23}$$

where $z=\eta_{0}$ is the position of the planar interface or thickness of the liquid layer, L_{L}, and $z=L$ is thickness of the combined solid–liquid system, $L=L_{\mathrm{s}}+L_{\mathrm{L}}$. For a small Λ, Λ^{-1} may be considered as the equivalent Biot number for heat transfer from the liquid to the solid [8]; also, Λ measures the amount of solid present in the system.

The surface boundary conditions become

$$@z=0,\quad T'_{\mathrm{L}}=0,\quad @z=1,\quad T'_{\mathrm{s}}=0. \tag{24}$$

Solution of the preceding set of equations results in a sufficient condition to ascertain the stability boundary of the particle-laden liquid layer. After eliminating the pressure from the liquid momentum equation by taking the curl twice and retaining only the z-component of the resulting equation yields

$$(1-\gamma)Pr^{-1}\frac{\partial}{\partial t}\nabla^{2}w+(1-\gamma)\nabla^{2}(\nabla^{2}w)-\Omega_{2}(\nabla^{2}w-\nabla^{2}s)+Ra(1-\gamma)\nabla_{H}^{2}T_{\mathrm{L}}=0, \tag{25}$$

where the primes have been dropped and s is the z-component of the particle velocity, v. Combining Eqs. (16) and (19a–c) thus eliminating v and T_{p}, produces

$$s=\varphi^{-1}L_{2}\{L_{3}u-(\nabla^{2}-\Omega_{1})T_{\mathrm{L}}\}-\Omega_{3}T_{\mathrm{L}} \tag{26}$$

for the particle velocity, and the thermal energy for the liquid region becomes

$$\varphi^{-1}L_{1}L_{2}\{L_{3}w-(\nabla^{2}-\Omega_{1})T_{\mathrm{L}}\}-\Omega_{3}L_{1}T_{\mathrm{L}}=RaT_{\mathrm{L}}\hat{k}-\Omega_{2}w. \tag{27}$$

The variables become separable under the normal modes assumption, yielding solutions of the form

$$\{T_{\mathrm{s}},T_{\mathrm{L}},w,\eta\}=\{g(z),f(z),\hat{w},\hat{\eta}\}\mathrm{e}^{\sigma t}\Phi(x,y), \tag{28}$$

where the time constant, $\sigma=\sigma_{\mathrm{r}}+\mathrm{i}\sigma_{\mathrm{i}}$, contains σ_{r}, the growth rate, and σ_{i}, the frequency of the disturbance, and $\Phi(x,y)$ is the plan form function which determines the cellular structure of the fluid motion and

satisfies the two-dimensional wave or membrane equation

$$\nabla_{\mathrm{H}}^2\Phi = -k^2\Phi. \tag{29}$$

Substitution of the normal modes into the linear perturbation model (Eqs. (15), (25) and (26)) results in the normal-mode disturbance equations for the solid

$$(D^2 - q)g = 0 \tag{30}$$

and for the liquid

$$(D^2 - q)^2\hat{w} + \frac{\gamma Ra}{1+\gamma}(D^2 - q)f - qRaf = 0 \tag{31}$$

and

$$\hat{w} = -\frac{1}{1+\varphi}\left(D^2 = q + \frac{Rc}{\Omega_2\Omega_3}\right)f, \tag{32}$$

where it has been assumed that the principle of exchange of stability is valid and the marginal stability curve is characterized by a growth rate of zero, i.e. $\sigma = 0$. This assumption is valid due to experience that the same analysis for the Bénard system is applicable for the addition of a solidification boundary as well as suspended particles [6,8,9]. The boundary conditions are transformed as

$$g(L) = 0, \quad g(1) = \frac{-\eta}{\Lambda} \tag{33}$$

for the solid region, and

$$\left.\begin{array}{llll} \hat{w}(0) = 0, & D\hat{w}(0) = 0, & f(0) = 0 & \\ \hat{w}(1) = 0, & D\hat{w}(1) = 0, & Df(1) = \Lambda Dg(1) & \end{array}\right\} \tag{34}$$

in the liquid region.

4. Solutions

4.1. Solid region solution

It is noticed that the general solution for the solidified layer may be obtained independent of the liquid equations, resulting in

$$g(z) = C_1\sinh(kz) + C_2\cosh(kz). \tag{35}$$

Use of the boundary conditions (Eq. (33)), yields the temperature profile in the solid as

$$g(z) = \frac{-\hat{\eta}\sinh[k(1+\Lambda - z)]}{\Lambda\sinh(k\Lambda)}. \tag{36}$$

4.2. Liquid region solution

Combining the disturbance equations (Eqs. (31) and (32)) in the liquid region eliminates the vertical velocity component, $\hat{w}$, and forms a single-variable perturbation equation in terms of the normal mode perturbation temperature, $f(z)$. Accordingly, the single-variable temperature perturbation equation transforms to a sixth-order, linear, homogeneous equation,

$$\begin{aligned}&(D^2 - q)^2(D^2 - qa)f(z) + qRa(1+\varphi)f(z)\\ &\quad + \frac{Ra\gamma}{1+\gamma}(1+\varphi)(D^2 - q)f(z)\\ &\quad = 0\end{aligned} \tag{37}$$

with six linear, homogeneous boundary conditions. Such conditions are determined by applying the solid solution and evaluating the continuity and thermal energy equations at $z = 0$, 1, given as

$$\left.\begin{array}{ll} z = 0, & f = (D^2 - qa)f = D(D^2 - qa)f = 0 \\ z = 1, & Df + k\coth[k\Lambda]f = (D^2 - qa)f = D(D^2 - qa)f = 0 \end{array}\right\} \tag{38}$$

where

$$a = 1 + \frac{2}{9}\Gamma^2\varphi\frac{Ra}{q}. \tag{39}$$

Note that in the limit of no particles ($\gamma = 0$ and $\varphi = 0$), and no solidification ($\Lambda = 0$), the system reduces to the governing system for a classical Bénard system with rigid boundaries. The sixth-order system constitutes an eigenvalue problem from which the onset of instability can be derived.

The essential task is to find the lowest occurring Rayleigh number, namely Ra_{c}, and wave number, namely k_{c}, for prescribed values of γ, φ, Γ and Λ which lead to a solution of $f(z)$ that satisfies the governing system. The critical parameters were determined parametrically using a shooting method in conjunction with a minimization program via a Runge–Kutta. integration method. For details of the numerical scheme, the reader is referred to Sparrow et al. [12].

In the asymptotic limits of $\Lambda = 0$ and $\Lambda \to \infty$ for $\gamma = 0$ the documented results of the critical Rayleigh and wave numbers of 1707.8 and 3.117 and 1492.815 and 2.815 for the classical Bénard system and the solidification analog [10], respectively, were recovered, thus validating the numerical scheme.

5. Results and discussion

The linear stability analysis has two experimentally

verifiable results: the critical temperature difference for the onset of convection and the corresponding critical wavelength. For a range of values for the particle concentration, γ, heat loading, φ, particle diameter ratio, Γ, and solid thickness, Λ, varying between limiting values, the incipient conditions for convection for a pure liquid solidifying in the presence of suspended particles are determined. The results are in terms of a reduced critical Rayleigh number, $r_c = Ra_c/1707.8$, and a reduced critical wave number, $\hat{k}_c = k_c/3.117$, where the parameters are scaled based on the classical solutions of the Bénard problem of 1707.8 and 3.117 for the critical Rayleigh and wave number respectively. The reduced critical Rayleigh numbers as a function of the heat loading, solid thickness and particle concentration appear in Figs. 2–4.

Figure 2 illustrates the destabilizing effects of the heat loading and the solid thickness. For the classical case of no particles ($\gamma = \varphi = 0$), it is shown that $r_c(\Lambda \to \infty) = 0.875$. This result is identical to those identified by Davis et al. [10] for a bulk liquid layer. However, increasing the heat loading in a system with a constant concentration of particles has a more pronounced destabilizing effect than the solid/liquid interface. Fig. 2 indicates that for a constant concentration of particles and various heat loading values, the solid thickness reduces the critical Rayleigh number 13% as the solid grows from zero to a ratio of 1; beyond which the values change by less than 1%. Moreover, it demonstrates that a 5% concentration of particles, heat loading of 100 and solid thickness ratio of one reduces the critical Rayleigh number nearly 85%, ($r_c(\Lambda \to \infty) = 0.1557$), severely destabilizing the system. A heat loading of 5 ($r_c(\Lambda = 0) = 0.885$), destabilizes the system on the same scale as that of increasing the solid thickness, $\Lambda \to \infty$. Thus, the system is sensitive to the thermal interactions of the liquid and the particles.

Figure 3 shows that for a system with no solidification the critical Rayleigh number is decreased by 40% with a particle concentration of 1%, which is consistent with theory [8]. When the particle concentration is increased from 1 to 5%, the stability is reduced by an additional 60% compared to the classical solution for the bulk liquid layer. Likewise, for the constant heat loading case, the increase in solid thickness decreases the stability by as much as 87.4% for the limiting case of $\gamma = 10\%$ and $\Lambda \to \infty$ ($r_c(\Lambda \to \infty, \gamma = 10\%) = 0.126$), compared to the 84% reduction for the previously stated case ($r_c(\Lambda \to \infty, \gamma = 5\%, \varphi = 100) = 0.1557$). For $\gamma = 1\%$, the reduction in stability is identical to that experienced in the classical Bénard case for $\Lambda \to \infty$, a reduction of 12.5%. However, a reduction of 13 and 14.7% is experienced in the critical Rayleigh number for 5 and 10%, respectively, as for $\Lambda \to \infty$.

The combined effects of the heating load and the particle concentration are displayed in Fig. 4. The heating has a strictly decreasing influence on the stability of the system for any concentration of particles. Scanlon and Segel [7] indicated that this was the sole reason for the destabilization, however, as the particle concentration increases in conjunction with an increasing heating load, the loss of stability is further pro-

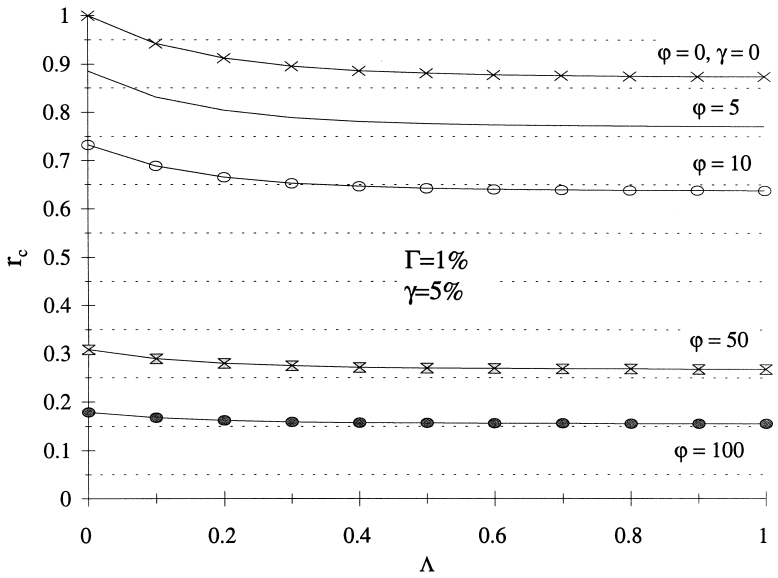

Fig. 2. Reduced critical Rayleigh number, r_c, vs. solid thickness, Λ, for $\gamma = 5\%$, $\Gamma = 1\%$.

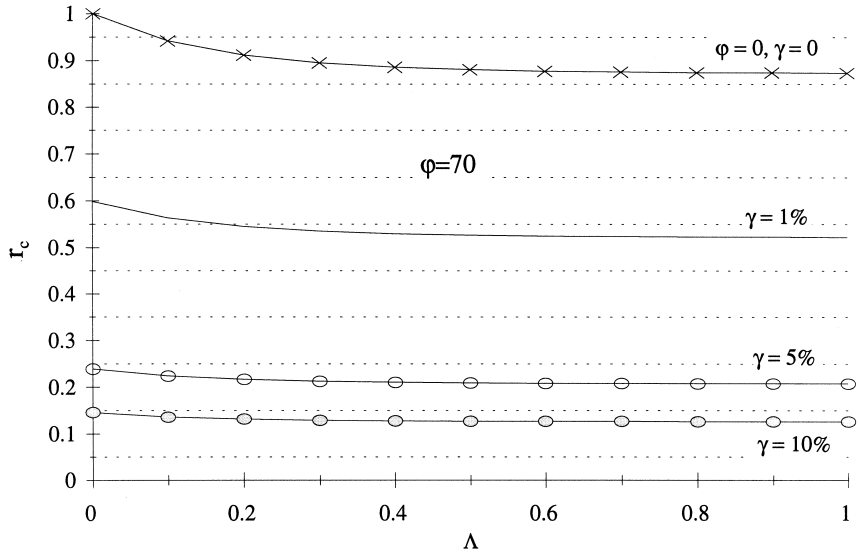

Fig. 3. Reduced critical Rayleigh number, r_c, vs. solid thickness, Λ, for $\varphi = 70$, $\Gamma = 1\%$.

nounced. Fig. 4 indicates that there is a 90% reduction in the critical Rayleigh number for $\Lambda = 3$, $\gamma = 10\%$, and $\varphi = 100$ ($r_c(\Lambda = 3) = 0.09$). A greater reduction results from an increase in particle concentration from 1 to 5%, compared to an increase from 5 to 10%.

While increasing the heat loading destabilizes the system, the particle diameter ratio, Γ, counters the trend for increasing values as observed in Fig. 5. These results are consistent with those of Rhazi et al. [8]. This result appears counter intuitive, as increasing the particle diameter ratio would seem consistent with increasing the concentration of particles which is destabilizing as shown in Fig. 5 and consistent with published results [7,8]. However, increasing the particle

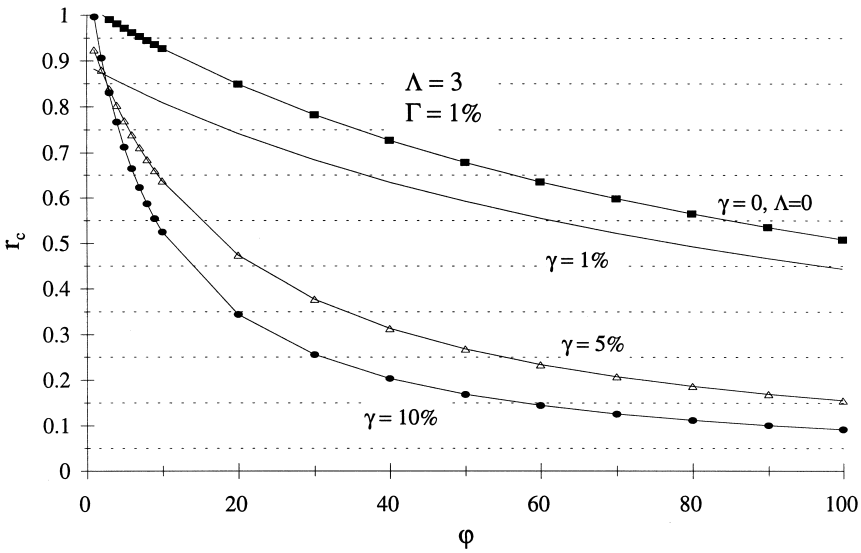

Fig. 4. Reduced critical Rayleigh number, r_c, vs. heat loading, φ, for $\Lambda = 3$, $\Gamma = 1\%$.

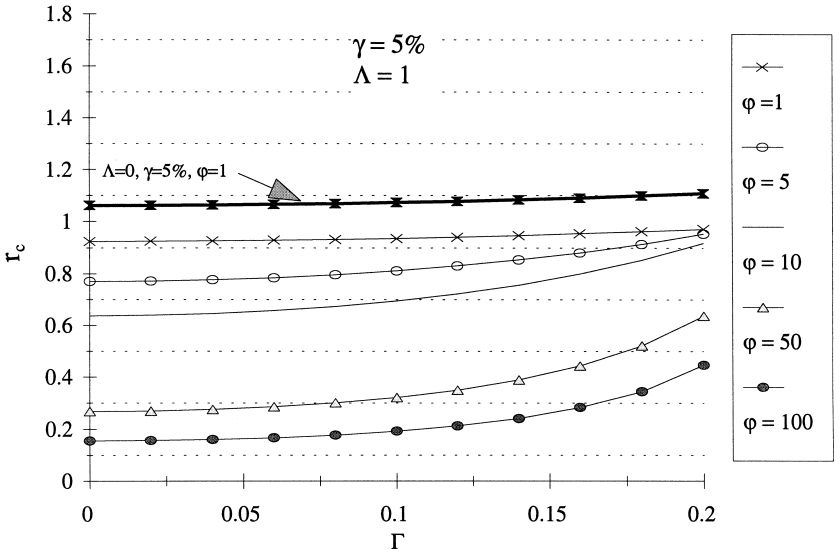

Fig. 5. Reduced critical Rayleigh number, r_c, vs. particle diameter ratio, Γ, for $\Lambda = 1$, and $\gamma = 5\%$.

diameter ratio may be considered like decreasing the layer thickness with a fixed concentration, which is analogous to increasing the permeability of a liquid saturated tortuous system which results in a stabilizing effect [11,13]. The destabilizing effect of the solid thickness is evident as Fig. 5 shows that for no solid, the system is more stable than the classical Bénard case. When the solid thickness is increased to a value of one, the system becomes less stable than the classical case for small ratios rising to the value of unity as the particle diameter ratio is increased.

The critical wave number is unaffected by the heat loading but Fig. 6 shows that the solid thickness ratio acts to decrease the size of cells whereas the particle

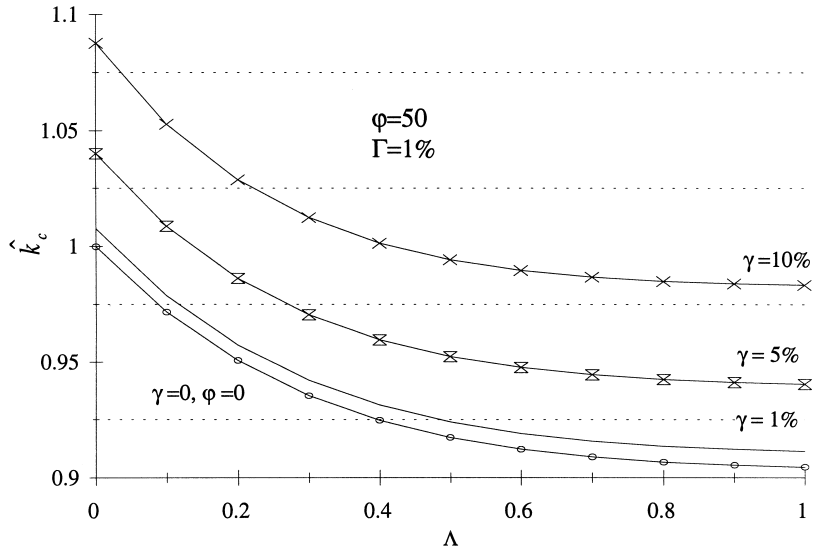

Fig. 6. Reduced critical wave number, k_c, vs. solid thickness, Λ, for $\varphi = 50$, $\Gamma = 1\%$.

concentration acts to increase the size. In the classical case of no particles and solidification, the size of the cells are reduced 10% in the limit $\Lambda \to \infty$. For $\gamma \geq 10\%$, the critical wave number is greater than that for the Bénard case independent of the amount of solid present as shown in Fig. 6. Fig. 7 shows plots of the critical streamlines and temperature eigenfunctions patterns for two-dimensional roll cells. At the onset of convection, Fig. 7a displays roll cells for the classical Bénard problem with no particles or solidification. Figs. 7b,c compared to the classical case display the effects of the initiation of growth of the solidification

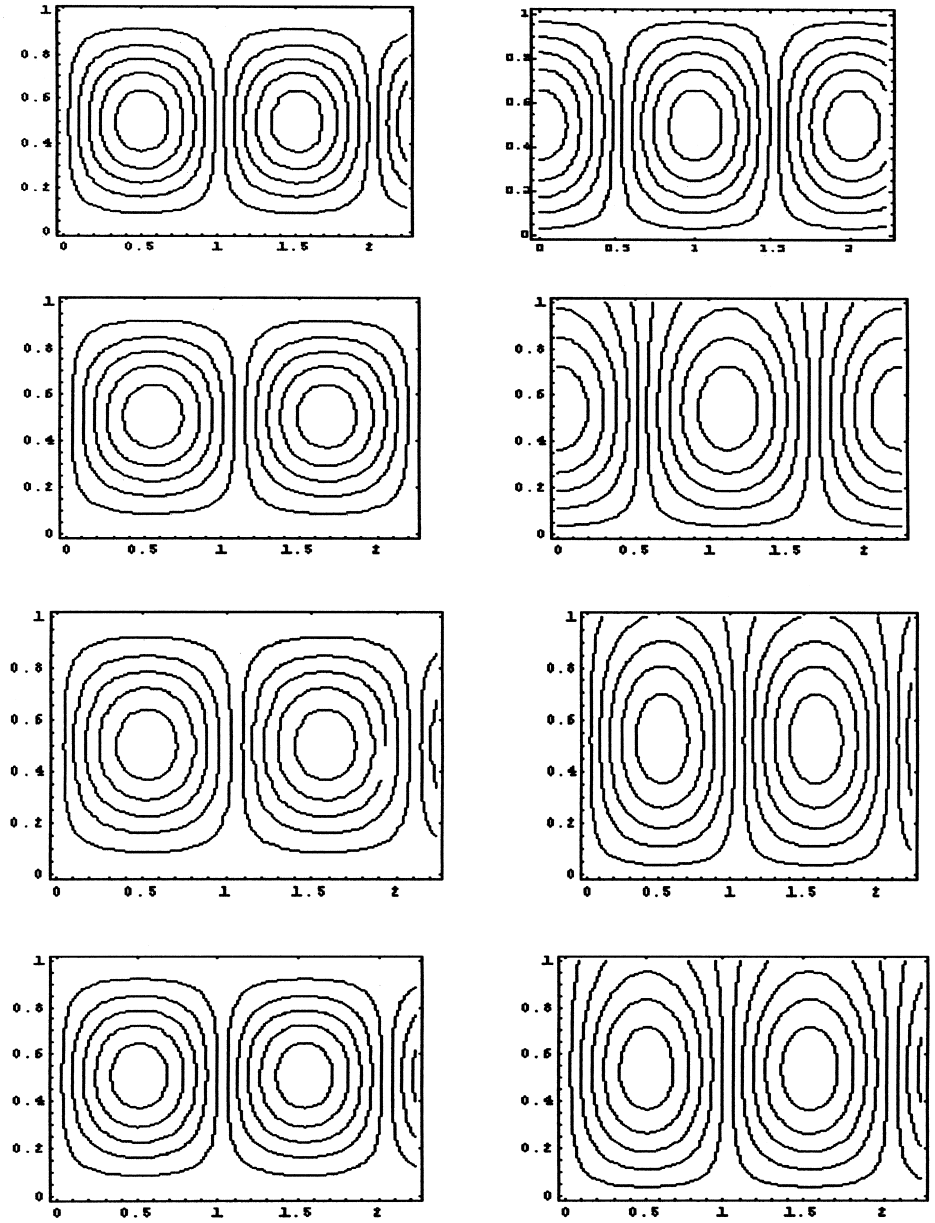

Fig. 7. Critical stream function and temperature eigenfunction respectively for different values of the φ, γ, Λ and Γ over one period. (a) $\varphi=0$, $\gamma=0$, $\Lambda=0$ and $\Gamma=0$; $Ra_c=1707.76$, $k_c=3.117$. (b) $\varphi=0$, $\gamma=0$, $\Lambda=3$ and $\Gamma=0$; $Ra_c=1492.65$, $k_c=2.815$. (c) $\varphi=50$, $\gamma=1\%$, $\Lambda=0.2$ and $\Gamma=1\%$; $Ra_c=1065.76$, $k_c=2.984$. (d) $\varphi=50$, $\gamma=1\%$, $\Lambda=3$ and $\Gamma=1\%$; $Ra_c=2891.17$, $k_c=3.0618$.

layer on the velocity and temperature contours. As this layer becomes thicker, the cells are constrained and decrease in size and the wavelength increases as shown in Figs. 7b,c where the wavelength, $\gamma = 2\pi/k_c$. Cells development is independent of heat loading and particle concentration and totally dependent on solid thickness established in Fig. 7. Mathematically, the solidification interface acts to slightly disrupt the vertical midplane symmetry of the system as confirmed by the departure of the temperature eigenfunctions from the symmetrical patterns in Figs. 7b–d when compared to Fig. 7a. Moreover, this phenomenon is demonstrated in the boundary conditions (Eq. (38)). As the solid becomes more pronounced the eigenfunctions become more deformed. Nonlinear theory is needed to further examine the effects of the solid thickness on the development of the motion beyond criticality.

6. Closing remarks

The introduction of particles in the solidifying systems has varying effects on the onset of instability of the system depending on different values. The heat loading has a greater effect on the stability of the system by increasing the effective heat capacity of the liquid. Thus, thermal disturbances are more readily diffused across the layer initiating thermoconvective motion. Along with heat loading, the concentration of particles decreases the threshold for the onset of nonlinear convection. When the particles and solidification of the system are considered together, the stability of the system or the potential for incipient convection is greatly increased. Experimentalists and manufacturers must concern themselves with the thermodynamic properties of additive particles as well as the concentration of such additions in any solidifying system. Convective motion of the liquid will not only further redistribute particles but will also assist in the development of a cellular interface; thus, decreasing the predictability of final distribution of particulates in such systems.

This study has considered the incipient convection of a liquid layer in the presence of suspended particles and solidification. The motion of the liquid not only affects the final distribution of the particles but also the interfacial traits of the solidifying material. This analysis has demonstrated that great care must be given to the possibility of incipient convection when all variables are considered. The results indicate that particles have a definite effect on the stability of the system and should be accounted for in any manufacturing or research inquiry.

Acknowledgements

The author is grateful for support for this work from the Louisiana Board of Regents — LEQSF/RCS.

References

[1] H. Huppert, The fluid mechanics of solidification, J. Fluid Mech. 212 (1990) 209–240.
[2] E.L. Koschmieder, in: Bénard Cells and Taylor Vortices, Cambridge University Press, New York, 1993, pp. 1–84 153–162.
[3] K.M. Fisher, The effects of fluid flow on the solidification of industrial castings and ingots, Physicochem. Hydrodynam. 2 (1981) 311–326.
[4] S. Chandrasekhar, Hydrodynamic and Hydromagnetic Stability, Dover, New York, 1961.
[5] P.G. Drazin, W.H. Reid, Hydrodynamic Stability, Cambridge University Press, New York, 1981.
[6] C. Sidbury, Effect of processing conditions on cast particulate reinforced composite materials, Ph.D. dissertation, Georgia Institute of Technology, Atlanta, GA, 1995.
[7] J.W. Scanlon, L.A. Segel, Some effects of suspended particles on the onset of Bénard convection, Phys. Fluids 16 (1973) 1573.
[8] M. Rhazi, A. Mir, Z. Zrikem, G. Gouesbet, Buoyancy driven convection in a particle–fluid mixture layer heated from below, Int. Commun. Heat Mass Transfer 22 (5) (1995) 705–712.
[9] C. Mackie, Convective instability in the presence of solidification and suspended particles, in: T.L. Bergman (Ed.), ASME Proc. of the 32nd National Heat Transfer Conference, vol. 9, HTD-Vol. 347, ASME, New York, 1997, pp. 47–55.
[10] S.H. Davis, U. Müller, C. Dietsche, Pattern selection in single-component systems coupling Bénard convection and solidification, J. Fluid Mech. 144 (1984) 133–151.
[11] C. Mackie, D. Prateen, C. Meyer, Rayleigh–Bénard stability of a solidifying porous medium, J. Heat Mass Transfer (1998) in press.
[12] E. Sparrow, W. Munro, V. Jonsson, Instability of the flow between rotating cylinders: the wide gap problem, J. Fluid Mech. 20 (1) (1964) 35–46.
[13] C. Mackie, Convective stability of a solidification interface in a porous layer, Ph.D. dissertation, Georgia Institute of Technology, Atlanta, GA, 1996.